International Symposium on Applied Geoinformatics (ISAG-2019)

A COMPARISON OF FEATURE SELECTIONS IN ALS POINT CLOUD CLASSIFICATION USING 3D NEURAL NETWORK

Eray Sevgen[1]*, Mehmet Onder Efe[2]

[1]Department of Geomatics Engineering, Hacettepe University, Beytepe, Ankara, Turkey
(eraysevgen@hacettepe.edu.tr); **ORCID 0000-0002-1682-4923**

[2]Department of Computer Engineering, Hacettepe University, Beytepe, Ankara, Turkey
(onderefe@hacettepe.edu.tr); **ORCID-0000-0002-5992-895X**

*Corresponding Author

ABSTRACT: Airborne Laser Scanning (ALS) point cloud classification is gaining its popularity corresponding with the increasing size of available ALS data in the last decade. While the classification is based on the different representation of the point cloud, such as top-view pixels or voxels, raw point cloud classification offers more detailed classification results; thus, it gives a better understanding of the three dimensional (3D) objects in the studied area. This study evaluates the performance of feature selection for ALS point cloud classification using 3D neural network classifier. The framework consists of three parts: i) feature extraction, ii) classification with neural network iii) quantitative evaluation of the classification results. The first part of the study includes feature extraction from the point cloud data. The feature extraction consists of three groups of features, namely, Light Detection and Ranging (LiDAR), geometry, and color based features. A LiDAR data have, in addition to its 3D information, intensity, which shows reflected energy from the ground object and multi-echo information, which defines the order of transmitting pulse. Height based features, which are dependent on the local neighborhood of the point, are also considered in the group of LiDAR features. Eigenvalues of a point define the geometry of the point; therefore, those feature descriptors form geometric features group. Airborne LiDAR data do not have color information, thus a true-orthophoto is used to get color information of each point in the point cloud. In the second part of the study, feature groups trained and tested using a conventional 3D neural network with stochastic gradient descent optimization algorithm. A data augmentation technique is applied before training in order to improve classification results and to prevent from class imbalance problem. The classification is performed on four urban classes, named as ground, building, tree, and car. At the last part of the study, quality metrics are calculated for each group of features and the results are compared with each other. According to the results, it is observed that LiDAR with color features has better accuracy with respect to geometric features.

Keywords: *Airborne Laser Scanner, LiDAR, 3D neural network, Feature extraction, Classification*

,

1. INTRODUCTION

LiDAR (Shan and Toth, 2018) is one of the popular data source of topographic mapping due to its capability of collecting direct 3D data in a short time and having advantages that are more rigorous in homogenous areas and being able to represent objects that are more detailed in 3D with respect to photogrammetric point clouds. It is basically based on the calculation of the distance between the object and the platform using the elapsed time between sending and transmitting pulse. While LiDAR systems can be mounted on terrestrial or mobile platforms, in this study, LiDAR data which was collected on the airborne platform is used. More properties of a LiDAR sensor can be found in Shan and Toth (2018).

The goal of classification in the point cloud is to categorize each representation unit (point, image cell, or voxel) to a meaningful group. Because of the unordered structure and having heterogeneous point density, point cloud classification can be considered as a challenging task. While many solutions exist for this task in the literature (i.e., Nguyen and Le, 2013; Grilli et al., 2017), machine learning methods using LiDAR point clouds has been gaining interest in the last decade. Features are playing a key role in those methods; therefore, the performance of the method is highly influenced by the derived features. This study presents the analysis of the performance of the feature selection for 3D neural network classifier based on the different group of features. The first group of features is derived from LiDAR point clouds, based on LiDAR's point's multi-echo, intensity, and height-based features in the local neighborhood. The second group of features includes geometric properties of each point in the local neighborhood. The third group of features cannot be extracted from LiDAR, therefore a true orthophoto is used. The point cloud an onto the orthophoto and the band values for each point are extracted. Lastly, all features are merged, and they form a group of features. Those four groups of features are classified in a single hidden layer neural network. More details for the methodology and details of implementation with the quantitative results are given in the next sections.

2. RELATED STUDIES

Machine learning has been intensively used for LiDAR point cloud classification in the literature. Random forest (Chehata et al., 2009; Canaz Sevgen, 2019; Blomley and Weinmann, 2017) Support Vector Machine (Zhang et al., 2013; Lodha et al., 2006) algorithms are studies for LiDAR data classification. The key factor in those algorithms is the feature selection. In other words, the classification accuracy is mainly based on selecting proper features. For instance, in Chehata et al. (2009) the height difference is found as the most influenced factor in the classification of an urban area. On the other hand, the representation of the point cloud is another factor in the classification. Generally, LiDAR point clouds are projected onto the grid surface from the top-view and feature images are created. Although, feature image-based point cloud classification mainly preferred in the literature, some information loss is unavoidable because of the representation. Other researchers used multi-view images (Boulch et al., 2017), where different angles used for feature image generation, or voxels (Engelche et al., 2016; Wang et al., 2018), where a 3D grid-based representation is created. In addition to feature images, some researchers used point-based classification (Yastikli and Cetin, 2016; Blomley and Weinmann, 2017). Qi et al. (2017) proposed an end-to-end deep learning framework in the literature where the features are extracted through the layers of the framework. In this study, however, the objective is to compare different features' classification performance in the 3D neural network classifier.

3. METHODOLOGY

According to the flowchart given in Fig. 2. the framework composed of three stages. At the first part, LiDAR, geometric and color feature are extracted. Secondly, a 3D neural network is trained and tested for the classification performance of the features. At the last stage, the results are evaluated quantitatively.

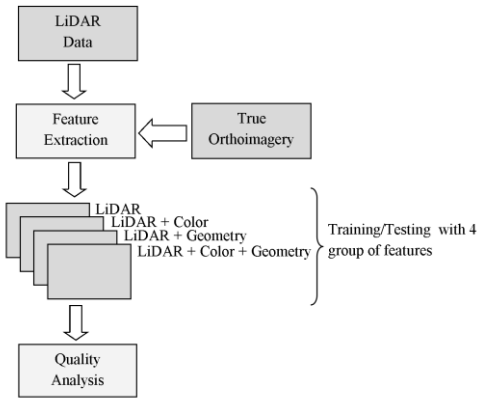

Figure.1 The flowchart of the study

Feature extraction consists of three groups of features. The first features include pure LiDAR properties, which are 3D coordinates, multi-echo, intensity, and height based features. Height-based and two intensity features, standard deviation and mean, are based on the neighborhood of the points. Table 1 summarizes the features for LiDAR group.

Table 1 LiDAR Features

Feature	Description
x,y,z	3D coordinate component of each point
I, $\boldsymbol{\sigma_I}$, μ_I	The intensity of a point
r,n	Number of returns and return number
e	Number of return over the number of total returns
$\boldsymbol{\sigma_H}$, $\mathbf{min_H}$	The standard deviation and minimum of heights in the neighborhood of a point
$\boldsymbol{\Delta_H}$, $\boldsymbol{d_H}$	The height differences in a points local neighborhood

Geometric features, on the other hand, are totally derived from the neighborhood of the points in ALS point cloud. The calculation is based on a neighbor search and eigenvalue decomposing from the covariance matrix. Eigenvalues, $\lambda_1 < \lambda_2 < \lambda_3$ are the results of the principal component analysis. The summary and derivation of the geometric features are given in Table 2.

,

Table 2 Geometric features

Feature	Description
Sum of Eigenvalues	$\boldsymbol{\lambda_1 + \lambda_2 + \lambda_3}$
Omnivariance	$\sqrt[3]{\boldsymbol{\lambda_1 \lambda_2 \lambda_3}}$
Eigenentropy	$-\sum_{i=1}^{3} \boldsymbol{\lambda_i \ln(\lambda_i)}$
Anisotropy	$\boldsymbol{(\lambda_1 - \lambda_3)/\lambda_1}$
Linearity	$\boldsymbol{(\lambda_1 - \lambda_2)/\lambda_1}$
Planarity	$\boldsymbol{(\lambda_2 - \lambda_3)/\lambda_1}$
Sphericity	$\boldsymbol{\lambda_3/\lambda_1}$
PCA1	$\boldsymbol{\lambda_1/\lambda_1 + \lambda_2 + \lambda_3}$
PCA2	$\boldsymbol{\lambda_2/\lambda_1 + \lambda_2 + \lambda_3}$
Surface Variation	$\boldsymbol{\lambda_3/\lambda_1 + \lambda_2 + \lambda_3}$
Verticality	$\boldsymbol{1 - \lvert\langle[0\ 0\ 1], e_3\rangle\rvert}$
Roughness	Distance to best-fitting plane

ALS does only have the intensity that represents the energy of the reflected object on the ground, but do not have color information. Because of this reason, color features are extracted from a true orthophoto. The combination of those features, such as standard deviation and mean, are calculated using the neighborhood of the points. Pseudo NDVI (Normalized Difference Vegetation Index) (Rottensteiner et al., 2003), however, calculated using LiDAR intensity and orthophotos green band. The summary of color features is given in Table 3.

Table 3 Color features.

Feature	Description
R,G,B	Red, green, blue values from true-orthoimages
$\boldsymbol{\sigma_R, \sigma_G, \sigma_B}$, $\boldsymbol{\mu_R, \mu_G, \mu_B}$	The standard deviation and the mean of red, green and blue bands in a local neighborhood of a point
pNDVI	Pseudo NDVI

At the classification part, the aforementioned four groups of features (Fig. 1) are the input of the neural network classifier. The neural networks have one hidden layer with the activation function of relu (Eq. 1), and the output layer has softmax (Eq. 2) activation with a cross-entropy loss function (Eq. 3) for each group.

$$relu(x) = \max(x, 0) \tag{1}$$

$$softmax(x_i) = \frac{e^{x_i}}{\sum_{j=1}^{n} e^{x_j}} \tag{2}$$

$$Loss(t_c, y_c) = -\sum_{c=1}^{M} t_c \log(y_c) \tag{3}$$

where n refers to the number of classes, t_c is the target class and y_c is the estimated class in the loss function, and M is the number of classes.

A schematic representation of the neural networks is depicted in Fig. 3. Note that for each group number of hidden layer's neuron is double of the number of neurons in the input layer. For instance, for the first group of features, the input layer has 11 features; therefore, the number of neurons in the hidden layer is 22 in this case. The output layer's neuron size is 4 for all feature groups. The parameters for the groups are identical; thus performance evaluation is in the same environment. Gaussian noise with 0 mean and 0.001 standard deviations is added to each feature in order to augment the training data set. Testing the classifier does not include any data augmentation.

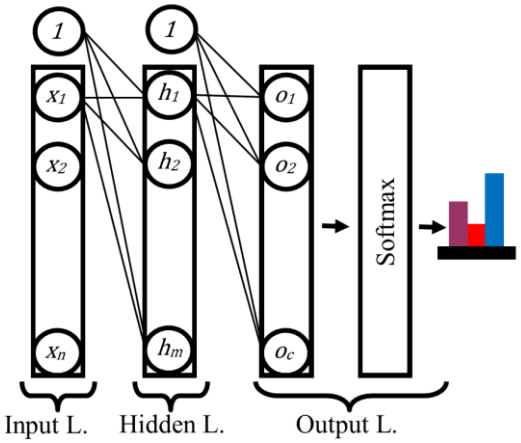

Figure.2 Proposed neural network

The quality analysis in this study is based on commonly used classification metrics, precision (Eq. 4), recall (Eq. 5) and F1-score (Eq. 6). Confusion matrix for each group's results is also given for better evaluation, specifically to interpret misclassification between classes.

$$Precision = \frac{TP}{TP + FP} \tag{4}$$

$$Recall = \frac{TP}{TP + FN} \tag{5}$$

$$F1\ Score = \frac{2 * Precision * Recall}{(Precision + Recall)} \tag{6}$$

4. IMPLEMENTATION AND DISCUSSION

Python programming language is selected as the programming language of this study because of its enormous support for machine learning libraries. Keras with Tensorflow backend is the main library for neural network implementation. In addition to that, manual labeling and geometric feature extraction are performed in CloudCompare, which is an open-source 3D data analyzing software. The ALS point cloud data is obtained from General Directorate of Mapping of Turkey. The data set collected in 2014 and available to research purposes. The true-orthophoto is obtained from General Directorate of Geographic Information Systems of Turkey. Its acquisition date is 2016. The study area of the presented study is Bergama, Izmir, Turkey (Fig. 4). The LiDAR data consist of approximately 1.2 million points and they split as training (75%) and testing (25%) sites as shown in Fig. 5.

,

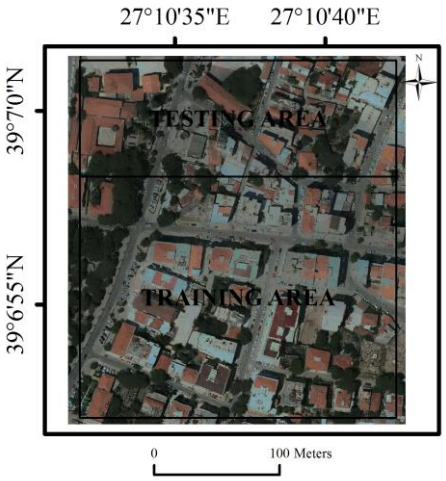

Figure.3 The study area located in Bergama, Izmir, Turkey.

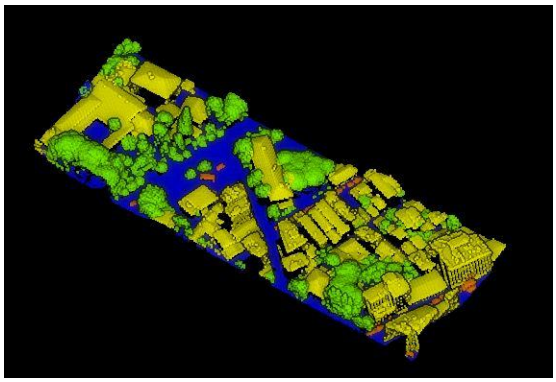

(a)

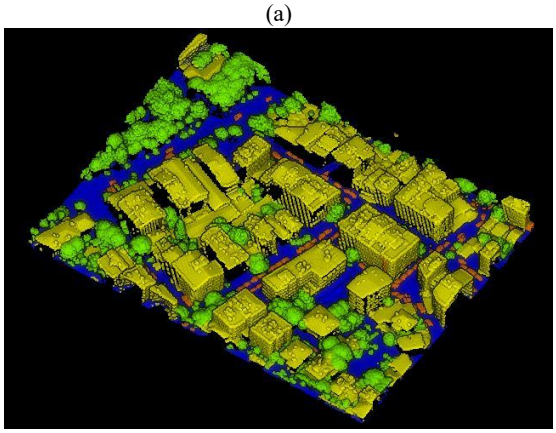

(b)

Figure.4 The ground truth of testing (a) and training (b) areas in 3D view.

After feature extraction and data augmentation, each group of feature is trained using stochastic gradient descent optimization with 0.005 learning rate, 128 batch size, and 0.9 momentum term. The number of epoch for the training is picked as 100 to let the neural network to reach its optimum results. Confusion matrix for each group and overall quality metrics are given in Figure 6 and Table 4, respectively.

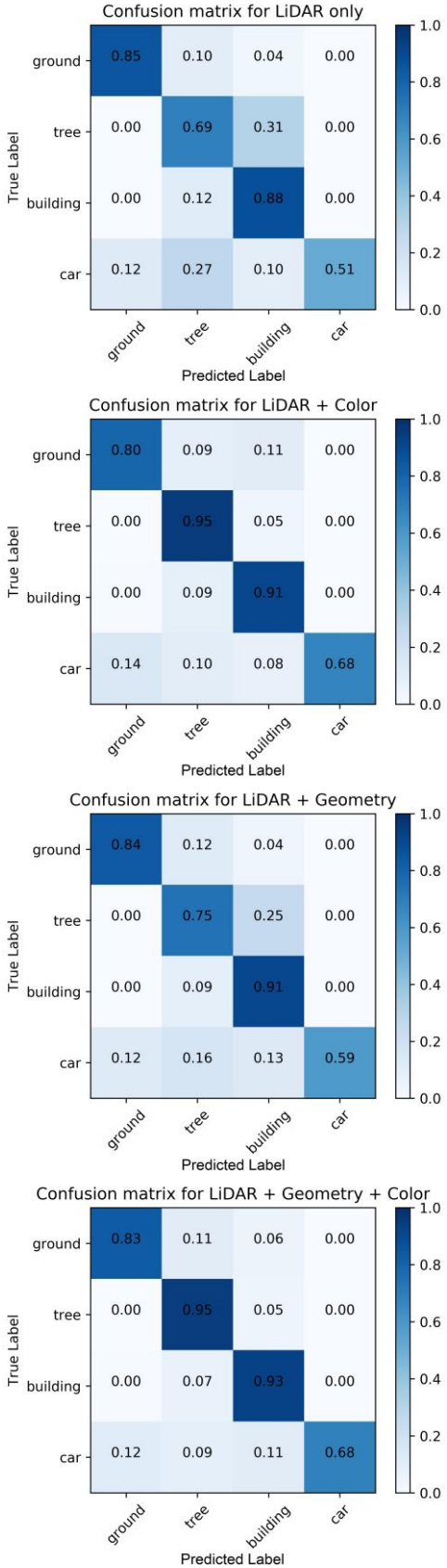

Figure.5 Confusion matrices, from top to bottom: Only LiDAR, LiDAR and Color, LiDAR and Geometry, All features.

,

Table 4 Quality metrics for the results

Feature Group	P*	R**	F1***
LiDAR	0.81	0.73	0.76
LiDAR+Color	0.86	0.83	0.84
LiDAR+Geometry	0.84	0.77	0.80
All features	0.87	0.85	0.86

*Precision, **Recall, ***F1-Measure

According to the results, the neural network is capable of extracting most of the objects in the study area. However, the main factor for the classification accuracy is the data augmentation where it was added to training data before performing training. Without data augmentation, small classes, such as car class, was not able to classify properly. In addition, car class still have mislabeled with an almost equal portion with other classes. One of the reason is that the study has complex structures; another reason is that the complexity of the network and the number of features is not enough to extract car classes. On the other hand, building class has the best accuracy almost in all feature groups. The difference from pixel-based approaches is that because we are studying point level classification, building class results can be used for building modeling for further studies.

Four groups of features have similar results with respect to each other, the last group that includes all features has the best overall scores. The reason is that the more features it has, the better the results are to obtain, as expected. However, it should be noted that color features are contributing more than other features in the overall best accuracy, even though the temporal accuracy of true-orthophoto and LiDAR is a bit different. Instead of using all feature in a large network, one can use only color features and have closer to the best results in terms of classification accuracy.

Overall, in this study, the accuracy performance of features is studied. According to the results, a neural network, as a powerful tool, is capable of separating many objects on the ground in airborne LiDAR data. However, the features need to be carefully selected. In the future, features can be expanded, as well as deep learning methods can be tested and compared with those hand-crafted features based neural networks.

ACKNOWLEDGMENTS

Authors thank to General Directorate of Mapping of Turkey and General Directorate of Geographic Information Systems of Turkey for sharing Bergama LiDAR data set and true-orthophoto for research purposes.

REFERENCES

Blomley, R. and Weinmann, M. (2017). Using multi-scale features for the 3d semantic labeling of airborne laser scanning data. ISPRS Annals of the Photogrammetry Remote Sensing and Spatial Information Sciences, Volume IV-2/W4.

Boulch, A., Le Saux, B., Audebert, N. (2017). Unstructured point cloud semantic labeling using deep segmentation networks, Eurographics Workshop on 3D Object Retrieval (3DOR), Lyon, France, pp. 17-24.

Canaz Sevgen, S. (2019). Airborne LiDAR data classification in complex urban area using random forest: A case study of Bergama, Turkey. International Journal of Engineering and Geosciences, 4 (1), pp. 45-51.

Chehata, N., Guo, L., Mallet, C. (2009) Airborne LiDAR feature selection for urban classification using random forests. International Archives of Photogrammetry Remote Sensing and Spatial Information Sciences, 39 (Part 3/W8), pp. 207-212.

Engelcke, M., Rao, D., Zeng Wang, D., Hay Tong, C., Posner, I. (2016). Vote3Deep: Fast object detection in 3D point clouds using efficient convolutional neural networks, IEEE International Conference on Robotics and Automation (ICRA), Singapore, pp. 1355-1361.

Grilli, E., Menna, F. and Remondino, F. (2017). A review of point clouds segmentation and classification algorithms. The International Archives of the Photogrammetry, Remote Sensing and Spatial Information Sciences, Nafplio, Greece, Vol. XLII-2/W3.

Lodha S. K., Kreps, E. J., Helmbold D. P., Fitzpatrick, D. (2006). Aerial LiDAR data classification using Support Vector Machines (SVM), Third International Symposium on 3D Data Processing, Visualization, and Transmission (3DPVT'06), Chapel Hill, NC, USA, pp. 567-574.

Nguyen, A. and Le, B. (2013). 3D point cloud segmentation: A survey, Proceedings of the IEEE Conference on Robotics, Automation and Mechatronics (RAM), Manila, Philippines, pp. 225–230.

Qi, C. R., Yi, L., Su, H., Guibas, L. J. (2017) PointNet++: Deep hierarchical feature learning on point sets in a metric space. Proceedings of the 31st International Conference on Neural Information Processing Systems, Long Beach, CA, USA, pp. 5105-5114.

Rottensteiner, F., Trinder, J., Clode, S., Kubik, K. (2003). Building detection using LiDAR data and multispectral images, DICTA, pp. 673-682.

Shan, J. and Toth, C. (2018). Topographic laser ranging and scanning, 2nd edn., CRC Press, Boca Raton.

Wang, L., Huang, Y., Shan, J., He, L. (2018). MSNet: multi-scale convolutional network for point cloud classification. Remote Sensing, 10 (4), 612.

Yastikli, N. and Cetin, Z. (2016). Classification of LiDAR data with point based classification methods, The International Archives of the Photogrammetry, Remote Sensing and Spatial Information Sciences, Volume XLI-B3, XXIII Congress, Prague, Czech Republic, pp. 441-445.

Zhang, J., Lin X., Ning, X. (2013). SVM-Based classification of segmented airborne LiDAR point clouds in urban areas. Remote Sensing, 5 (8), pp.3749–3775.

International Symposium on Applied Geoinformatics (ISAG-2019)

EXTRACTION OF HIGHWAY GEOMETRY PARAMETERS FROM AIRBORNE LIDAR DATA AND IMAGERY

Baris Suleymanoglu [1]*, Metin Soycan[1]

[1]Yildiz Technical University, Faculty of Civil Engineering, Department of Geomatics, Istanbul, Turkey
(bariss/soycan@yildiz.edu.tr)

*Corresponding Author

ABSTRACT: Road surface and its surroundings are used to generate road inventory information such as on-road information (road surfaces, road signs, roadside), roadside information (traffic signs, light pole, trees) and geometric elements (road cross section, horizontal and vertical alignment, sight distance assessment). Road inventory information can be used variety of application such as intelligent transportation system (ITS), urban planning, 3D digital city modeling, generating high-definition roadmap, architecture and façade measurement and civil engineering. Data obtained from different surveying techniques can be used to generate road inventory information. These methods and systems include classical geodetic methods (GPS, Total Station), satellite imagery, aerial and terrestrial photogrammetric techniques and lidar (air, mobile and terrestrial) systems. These systems may have different advantages and disadvantages. To overcome this, data obtained from different systems should be used. In this study, data obtained from two different systems such as airborne lidar and photogrammetric system were used. In this study, it is aimed to extract and detect on-road information (road surfaces, road signs and roadside) and calculating geometric parameters of the road by using Airborne Lidar (ALS) data and orthophoto. It is aimed to determine road surface and boundaries by using ALS data and detect lanes on the road surface by using orthophoto. Road lane markings were extracted from orthophoto using image processing techniques. The road centerline points were extracted by vectorizing the lane lines. Afterward, filtering were performed in order to clean non-ground objects in ALS data. So, the objects around the road were filtered to facilitate the determination of the road surface and increase the accuracy. Thereafter, cross-sections were taken using road centerline points within filtered lidar data. In order to find points of road axis each cross-section is divided into grid parts. The curve fitting method was applied to the points in each section and the points of road axis were determined from the intersection of fitting lines. Using these point information geometrical elements of highway such as cross-sectional and longitudinal slopes were calculated.

Keywords: *Road Detection, Airborne Lidar, Road Geometry, Remote Sensing*

,

1. INTRODUCTION

Establishment of an advanced transport network and infrastructure is very important for the economic and social development of the country. Information about transportation features is required for management, security controls and maintenance of assets of roads. These features divided into three categories: on-road features (road surface, road edges, road lane and marking), roadside features (traffic sign and lamps, pole-like objects) and geometric design parameters (horizontal and vertical alignments, cross and longitudinal slope) of the roads (Gargoum and Basyouny, 2019). The existence of this information is a necessity for carrying out a large number of analyzes and applications. To illustrate these, information on road surface and boundaries plays a crucial role in the development of intelligent transportation systems, urban planning studies, 3D city modeling and creation of high-resolution maps (Yu et al., 2014). Road marking (zebra crossings, direction arrow) and lane lines provide necessary road information for all road users. Road markings are essential for advanced driver assistance system and planning navigation routes to prevent collision of driverless vehicles on busy roads and ensure safe driving (Ma, 2018). Geometric design parameters of the road are very important for the analysis of road safety, road expansion and infrastructure studies (Higuera de Frutos and Castro, 2017). Horizontal alignment are designed to allow vehicles to cross curves safely (Gargoum et al., 2018b). Vertical alignment are important for safety studies such as visibility. In this context, it is very important to calculate the geometric data of the road (Gargoum et al., 2018).

In this study, it is aimed to detect and extract road surface, edges and boundaries. For this purpose, the process shown in Fig. 2 was carried out respectively. Firstly, lane lines were detected and vectorized from the orthophoto and points of these lanes were extracted. Afterwards, these points are used as road centerline points of the road and the points of the road boundaries are extracted from the airborne lidar data and the information about road geometry was calculated. For this purpose, filtering process was performed in order to filter non-ground objects in point cloud data. Afterwards, raw filtered data from this data were used to determine the road boundaries. Cross sections were created using road centerline points that generated from the orthophoto. In order to find points of road axis **e**ach cross-section is divided into grid parts**.** The curve fitting method was applied to the points in each section and the points of road axis were determined from the intersection of fitting lines. Finally, using these points, lane boundary, longitudinal and cross slope information and cross-sectional parameters were obtained.

2. MATERIAL AND METHODS

2.1 Test Areas and Data

In this study, ALS data and orthophoto were used to extract and detect on-road information and calculating some geometric parameters. These data were obtained from Evrencik County of Kirklareli Province of Turkey. Lidar system was used to obtain this data. The examples of test area are shown in Fig.1.

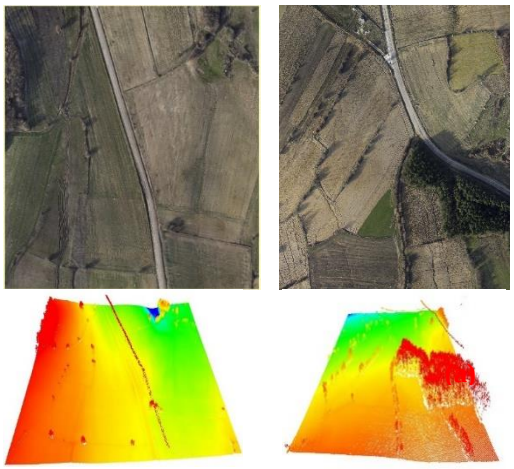

Figure.1 The examples of test area.

2.2 Processsing Methodology

Processing steps for detecting lane points from images (orthophoto) were shown in Fig. 2. Firstly, an input georeferenced image was converted into a grayscale image. Grayscale image is one in which that each pixel contain only intensity information (Johnson, 2006). In the next step, binary images were generated from grayscale images. Binary images are digital images that each pixel has two possible values and stored as a single bit 0 or 1. In general, black and white colors are used to visualize binary images. In this study, binary images are generated with the thresholding. There are different approaches for the generation of binary images such as segmentation, thresholding and dithering (Shapiro et al., 2002). In this study, thresholding approach was used to generate binary image. In its simplest form, the thresholding methods determines each pixels color by comparing pixel intensity values ($I_{i,j}$) to some fixed constant threshold. If the compared pixel is smaller than the threshold, that pixel is visualized with black, otherwise white (Shapiro et al., 2002). After the grayscale image was converted to a binary image and some salt-and-pepper noise occurred on the image as shown in Fig. 3(c). The median filter is used to reduce noise in an image. In order to do that median filter use pixel's neighborhood. The pixel value is changed by taking the middle value by sorting the neighboring pixels (Szeliski, 2010). Lastly, road centerline vectorization done by using line approximation algorithms that generate vector lines using pixel's location (Chiang et al., 2013).

,

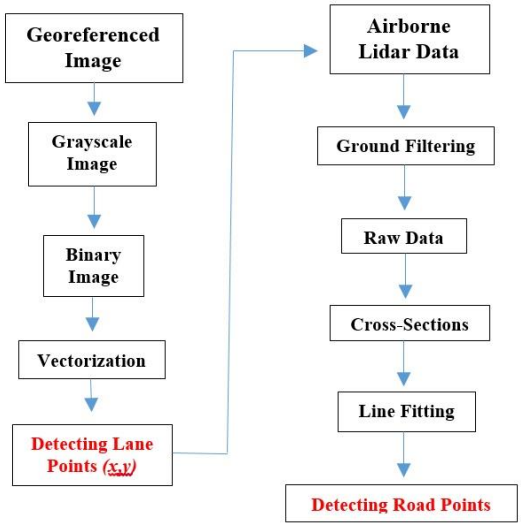

Figure.2 Workflow applied for lane detection from Images

Figure.3 illustrated the results of the operations performed during the process of determining the road center point from the images using the methodology described above.

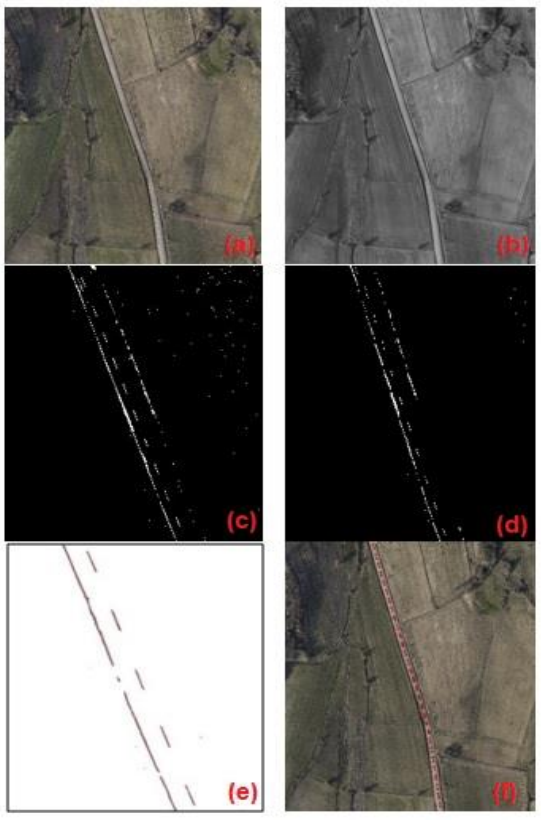

Figure.3 (a) Orthophoto (b) Grayscale (c) Binary Image (d) Median Filter (e) Vectorization (f) Lane Points.

After road centerline points were determined from the orthophoto, longitudinal sections of roads created using these points. Besides, same road centerline were manually digitized. Reference longitudinal sections were created using these points.

Reference longitudinal section profile was generated by using manually digitized road centerline points as shown in Fig. 4 (b), test longitudinal sections created from extracted lane points as shown in Fig. 4 (c). As can be seen from the figure, results were very close to each other. The height differences of reference longitudinal section was 13.65 m and slope value was % 4.25. Height differences of tested longitudinal section was 13.79 m and slope value was % 4.29. When all these results are examined, it is seen that the points obtained from the images are very successful in representing the road centerline.

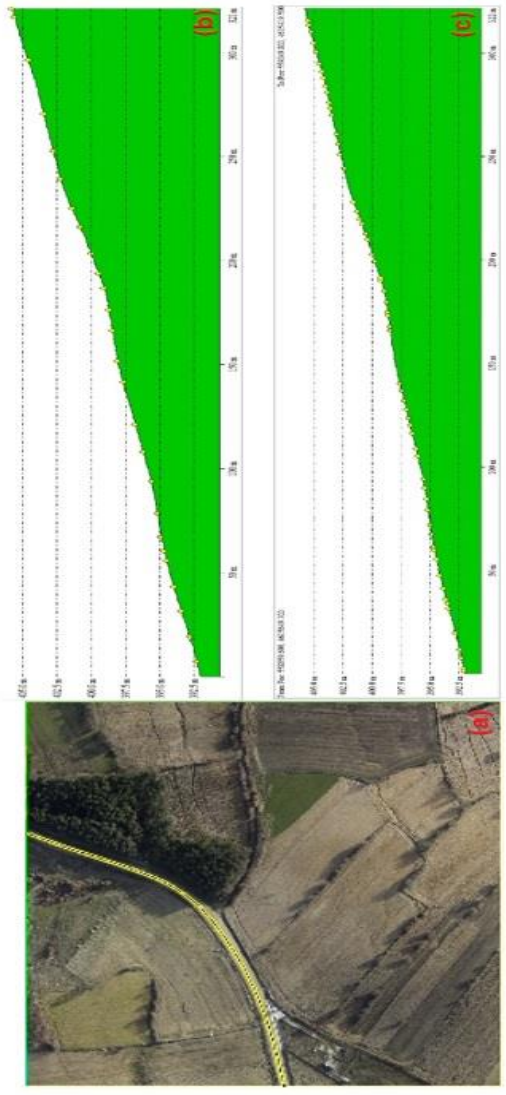

Figure.4 (a) Test area, (b) Reference, (c) Test Longitudinal Section.

,

After detecting and extracting points of road centerlines from the images, road boundaries, shoulders and ditches of the road were determined from ALS data. In order to do this, firstly, Lidar data was filtered to remove non-ground objects that would affect the accuracy of the method. After filtering, cross sections were taken along the road route using road centerline points. Along the cross-sections, the road was divided into certain parts from the mid-point to the right and left. A lines that best fit for every part were determined using linear fitting approach. Lastly, the points of road axis were determined from the cutting points of these lines as seen in Fig. 5. As shown in Fig. 5(a), cross-sections were taken along the road route using road center points obtained from the images. With the help of these cross-sections, center, edge and ditch point of road section were determined as shown in Fig. 5(c). The location of these points in the test area is shown in Fig. 5(b). Generally, 10 cm differences were calculated between actual and detected road edge and ditch points. It is expected that this accuracy will be further enhanced by improvements in methodology.

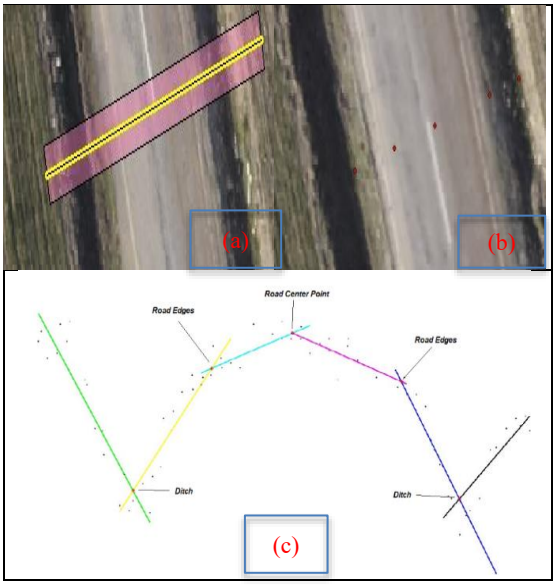

Figure.5 Road points extraction from cross-section.

3. CONCLUSION

As a result of the study, determination of the road boundaries by using orthophoto and ALS data, road lane line information, road boundary and road geometry information were extracted. However, it has been observed that accuracy varies depending on the some factors. Accuracy of detecting lane lines on the road surface from images, depend on absence of lane markings, quality of image and shadow effect. This affects vectorization of lane lines and road centerline points generated by this vectorization process. In addition, the accuracy of road point estimation can be increased by testing different curve fitting approaches. As a result, it is thought that the proposed methodology can be improved with all these arrangements.

REFERENCES

Johnson, Stephen (2006). Stephen Johnson on Digital Photography. O'Reilly. ISBN 0-596-52370-X.

Shapiro, Linda G. & Stockman, George C. (2002). "Computer Vision". Prentice Hall. ISBN 0-13-030796-3

Szeliski, Richard. Computer vision: algorithms and applications. Springer Science & Business Media, 2010.

Chiang, Yao-Yi, and Craig A. Knoblock. "A general approach for extracting road vector data from raster maps." International Journal on Document Analysis and Recognition (IJDAR) 16.1 (2013): 55-81.

Ma, Lingfei, et al. "Mobile laser scanned point-clouds for road object detection and extraction: A review." Remote Sensing 10.10 (2018): 1531.

Gargoum, S. A., El Basyouny, K. 2019. “A literature synthesis of LiDAR applications in transportation: feature extraction and geometric assessments of highways”, GIScience & Remote Sensing, 56(6), 864-893.

Yu, Y., Li, J., Guan, H., Jia, F., Wang, C. 2014. “Learning hierarchical features for automated extraction of road markings from 3-D mobile LiDAR point clouds”, IEEE Journal of Selected Topics in Applied Earth Observations and Remote Sensing, 8(2), 709-726.

Higuera de Frutos, S., Castro, M. 2017. “A method to identify and classify the vertical alignment of existing roads”, Computer-Aided Civil and Infrastructure Engineering, 32(11), 952-963.

Gargoum, S., El-Basyouny, K., Sabbagh, J. 2018b. “Automated Extraction of Horizontal Curve Attributes using LiDAR Data. Transportation Research Record”, 2672(39), 98-106.

Gargoum, S. A., El-Basyouny, K., Froese, K., Gadowski, A. 2018. “A Fully Automated Approach to Extract and Assess Road Cross Sections From Mobile LiDAR Data”, IEEE Transactions on Intelligent Transportation Systems, 19(11), 3507-3516.